

THE OOSTERHOFF PERIOD EFFECT: LUMINOSITIES OF GLOBULAR CLUSTER ZERO-AGE HORIZONTAL BRANCHES AND FIELD RR LYRAE STARS AS A FUNCTION OF METALLICITY

ALLAN SANDAGE

The Observatories of the Carnegie Institution of Washington

Received 1989 February 16; accepted 1989 August 17

ABSTRACT

The purpose of this paper is to determine the variation of absolute magnitudes of RR Lyrae stars with metal abundance by using the pulsation properties of the variables. It is shown again that the period ratios (expressed as differences in $\log P$, or “period shifts,” star by star) for the variables in one globular cluster relative to another at the same temperature are correlated with $[\text{Fe}/\text{H}]$. There is explicit discussion of the sensitivity of the correlation to errors in the adopted reddenings. The equivalent analysis of luminosity-to-mass ratios (rather than period shifts) for variables in 10 clusters and for the variables in the field studied by Lub reveal the correlation to be $\log(L/M^{0.81}) = -0.10[\text{Fe}/\text{H}] + 1.74$ —the same as found by Lub. This equation applies for RR Lyrae stars at the luminosity level that represents the average post-zero-age horizontal-branch evolutionary state. The relation for the zero-age horizontal-branch state is fainter by ~ 0.1 mag, reducing the constant to 1.70.

The Oosterhoff progression of the ensemble average RRab period in individual clusters is shown to be continuous with $[\text{Fe}/\text{H}]$, but exhibiting the Oosterhoff separation into two period groups with a period gap at $\log P(\text{days}) = -0.22$. The gap is caused by the nonmonotonic behavior of the morphology of the horizontal branch with progressive variation of $[\text{Fe}/\text{H}]$.

Combining the $L/M^{0.81}$ relation with several assumptions for the variation of mass with $[\text{Fe}/\text{H}]$, and applying the bolometric correction, gives $M_V(\text{RR}) = a[\text{Fe}/\text{H}] + b$, where a ranges between 0.19 and 0.39, and b between 0.86 and 1.17 mag, depending on a . The uncertainty in a depends on the adopted mass- $[\text{Fe}/\text{H}]$ relation which, at present, is largely not known with the necessary precision. The uncertainty in the zero point b is at least 0.2 mag because of uncertainties in (1) the constant in the pulsation equation, (2) the zero point of the color-temperature relation, and (3) the zero point of the mass scale. The value of a is the central issue, because it can be made to carry the cosmogonical burden of whether the age of the globular cluster system in the Galaxy depends on $[\text{Fe}/\text{H}]$ or is independent of it.

Subject headings: clusters: globular — stars: horizontal-branch — stars: luminosities — stars: RR Lyrae

I. INTRODUCTION

The subject of this paper is the absolute magnitudes of RR Lyrae stars as a function of their metallicities. The problem is related to the facts that (1) the Oosterhoff (1939, 1944) separation of globular clusters into two RR Lyrae period groups is a separation by cluster metallicity (Arp 1955; Kinman 1959); (2) this period-shift effect exists for each RR Lyrae star in a given cluster (Sandage, Katem, and Sandage 1981, hereafter SKS; Sandage 1981, 1982a, hereafter S81, and S82a) rather than being caused by differences in ensemble averages over different distributions of periods in different clusters (van Albada and Baker 1973; Stellingwerf 1975a; Caputo, Castellani, and Tornambè 1978), i.e., the Oosterhoff mean period difference between clusters is a star-by-star phenomenon; and (3) field RR Lyrae stars also show the period-shift-metallicity effect (Sandage 1982b, hereafter S82b, Fig. 1; Lub 1977, 1987), similar to that of the cluster variables.

The only explanation consistent with the $P\langle\rho\rangle^{1/2} = Q$ pulsation condition is that RR Lyrae stars that have longer periods than others of the same temperature also have a different luminosity-to-mass ratio. By inserting the observed data on temperatures and periods into the theoretical pulsation equation (van Albada and Baker 1971; Iben 1971; Cox 1987), and ignoring the mass variations, we concluded (SKS; S81, S82a)

that the observed period shifts require the RR Lyrae stars to differ in luminosity from cluster to cluster, depending on $[\text{Fe}/\text{H}]$. The sense of the difference is that clusters with the longest period variables at a given temperature must be brighter than variables of shorter period. The size of the magnitude difference is ~ 0.2 mag between clusters such as M3 and M15 which differ in the log of their average RR star periods by 0.07 dex and in their metallicity by 0.7 dex.

However, these observational results presented a problem when they were compared with the predictions of theoretical HB models such as those of Sweigart and Gross (1976) or Caloi, Castellani, and Tornambè (1978). The required dependence of the L/M ratio on metallicity could be achieved only by varying the helium abundance in the standard models. The sense of the variation is an *anticorrelation* of Y with $[\text{Fe}/\text{H}]$; the lower the metal abundance, the higher the helium abundance must be if the model stars are to give the observed dependence of pulsation periods on metallicity.

This anticorrelation required by the models has been verified now in an extensive literature (cf. Renzini 1983; Caputo, Cayrel, and Cayrel de Strobel 1983; Caputo, Castellani, and di Gregorio 1983; Tornambè 1985; Caputo *et al.* 1987; Sweigart, Renzini, and Tornambè 1987; Buonanno, Corsi, and Fusi Pecci 1988; Renzini and Fusi Pecci 1988), yet is so contrary to

intuition that one suspects either the theory or the reality of the supposed observational effect. From an exhaustive exploration of a number of possibilities for changing the theoretical input parameters, Sweigart, Renzini, and Tornambè (1987, hereafter SRT) conclude that there is as yet no satisfactory explanation of the period-shift effect within the standard theoretical frame except by anticorrelating Y and Z .

Because of this impasse, Caputo (1988) has suggested that the observed period-shift variation with metallicity may not be real, and therefore that our interpretation of the observations in 1981/1982 was wrong. She supposes that using the period-shift values measured at constant amplitude (as we did in part of the argument in S82a, b) may give a spurious variation of period shift with metallicity between clusters because amplitude at a given temperature may be a function of metallicity. The apparent correlation between $[Fe/H]$ and the period shifts derived at *constant amplitude* might then be an artifact of using such data. A similar argument is made by Lee, Demarque, and Zinn (1988, 1990, hereafter collectively LDZ) concerning the use of rise times to determine period shifts. And, although neither Gratton, Tornambè, and Ortolani (1986, hereafter GTO) nor LDZ argue for the *elimination* of the effect, they do argue for a reduction of its amplitude. They suggest that correcting the data in any given cluster to what would be observed on the ZAHB (i.e., by accounting for post-ZAHB luminosity evolution) could reduce the size of the resulting period-shift-metallicity correlation by about a factor of 2 from what we originally found (SKS; S81, S82a, b).

The problem with these criticisms is that to eliminate or to appreciably reduce the star-by-star period shifts between clusters of different metallicities turns a blind eye to the Oosterhoff variation of the ensemble average of the RR Lyrae periods from cluster to cluster. The mean periods *do* differ between clusters, varying systematically with $[Fe/H]$; and the clusters do divide into two period groups—the effect being the Oosterhoff (1939, 1944) period dichotomy. If, then, the period ratios at fixed temperature are not present *star by star* in one cluster relative to another with a value close to that determined in S82a, one would have to explain the Oosterhoff variation of *mean* RR Lyrae periods as a hysteresis in the transition between pulsation modes such as in the models of van Albada and Baker (1973), Stellingwerf (1975a), or Caputo, Castellani, and Tornambè (1978). As a consequence, one must then also fault that part of the demonstration in SKS, S81, and S82a where we used the period shifts determined at *constant temperature* on a star-by-star basis and found that these also were correlated with $[Fe/H]$.

Use of period shifts determined from temperature data, of course, makes moot the arguments of Caputo and of LDZ that rely on amplitude or rise-time data. For this reason, we make no use of amplitude and rise times for the main argument in the present paper. Rather, the *temperature* data are used directly to show again that the period-shift-metallicity relation is as large as originally derived (S81, S82a).

Caputo recognized, of course, that the color information in each of the clusters which we previously discussed argues *for* the reality of the period-shift-metallicity effect because the test is independent of data on amplitudes which she criticizes. Therefore, to make invalid that part of our previous demonstration of the period-shift dependence on $[Fe/H]$ that uses temperatures, she suggests that the reddening corrections we used in S82a are in error. The error would have to vary system-

atically with $[Fe/H]$ in such a way as to eliminate the derived cluster-to-cluster period-temperature shifts as a function of metallicity.

However, the field RR Lyrae data of Lub (1977, 1987) argue against this suggestion. Lub finds the same period-shift-metallicity relation for these field stars that we found between the clusters. His reddening values for the field variables are well determined. The period shifts (or the equivalent L/M ratios) can therefore be determined from the *temperature* and period data directly.

The purpose of the present paper is to address the cluster analysis again using only color and temperature data in the principal argument, and using masses obtained from (1) the application of pulsation theory to the observed P_0/P_1 period ratios for double-mode RR Lyraes or (2) the model of LDZ where no RR Lyraes in metal-poor clusters are on the ZAHB because of post-ZAHB evolution. In the next section we review the problem of the Oosterhoff period dichotomy itself. In § III we use the color and period data on cluster variables from the preceding paper (Sandage 1990, hereafter S90) to restudy the period-shift-metallicity relation and the equivalent L/M -metallicity relation for the zero-age horizontal branches in 10 program clusters. A strong correlation between $L/M^{0.81}$ and $[Fe/H]$ is found again, similar to that found in S81 and S82a. Confirmatory analysis using Lub's field star data is set out in § IV.

In § V we combine the correlation of $L/M^{0.81}$ and $[Fe/H]$, found in § IV, with the mass-metallicity relation obtained from the pulsational analysis of double-mode RR Lyraes found in clusters of different metallicity, and with other assumptions about the mass-metallicity relation. These various possibilities concerning the masses give a series of values for the variation of RR Lyrae absolute bolometric luminosity with metallicity.

In the final section the theoretical ZAHB models of SRT are shown, again, to require an anticorrelation of helium and metal abundance to explain the observations if the correlation applies to the ZAHB. The alternate suggestion of LDZ that metal-poor RR Lyrae stars are highly evolved from the ZAHB, and therefore that the ZAHB models do not apply, is also discussed here.

II. THE OOSTERHOFF PERIOD DICHOTOMY

Data on mean periods of the RRab Lyrae variables in clusters with adequate data are listed in Table 1. The data on periods are obtained by averaging the entries in Sawyer Hogg's (1973) Third Catalog of Variable Stars in Globular Clusters, updated from the more recent literature as listed in S82a (Table 1, col. [11]). (The literature reference to the periods in IC 4499, not given there, is Clement, Dickens, and Bingham 1979.) Column (4) shows the number of variables used to obtain the mean period that is listed in column (2). The metallicity shown in column (5) is from Zinn and West (1984).

All data with $n > 2$ are plotted in Figure 1a; the subset with $n > 9$ is shown in Figure 1b. The two features to note in Figure 1 are (1) the clear correlation of $\langle P_{ab} \rangle$ with $[Fe/H]$ and (2) the *gap* centered at $\log P = -0.22$ ($P = 0.6$ days). This separation into *two period groups* is the Oosterhoff period dichotomy.

Concerning point 1, the least-squares line shown in Figure 1b has the equation

$$\log \langle P_{ab} \rangle = -0.090[Fe/H] - 0.383, \quad (1)$$

TABLE 1
THE OOSTERHOFF PERIOD EFFECT AS A FUNCTION OF $[Fe/H]$

(1) Cluster	(2) $\langle P_{ab} \rangle$	(3) $\log \langle P_{ab} \rangle$	(4) n	(5) $[Fe/H]_{zw}$	
NGC362	0.542	-0.266	7	-1.27	
1261	0.563	-0.249	10	-1.31	
1851	0.573	-0.242	14	-1.36	
2419	0.650	-0.187	19	-2.10	
3201	0.558	-0.253	69	-1.61	
4147	0.525	-0.280	6	-1.80	
M68	4590	0.625	-0.204	14	-2.09
4833	0.684	-0.165	6	-1.86	
M53	5024	0.633	-0.199	18	-2.04
5053	0.672	-0.173	5	-2.58	
ω Cen	5139	0.653	-0.185	76	-1.59
M3	5272	0.551	-0.259	148	-1.66
5824	0.624	-0.205	7	-1.87	
5466	0.637	-0.196	11	-2.22	
IC	4499	0.578	-0.238	52	-1.50
M5	5904	0.547	-0.262	67	-1.40
M4	6121	0.538	-0.269	30	-1.33
M107	6171	0.527	-0.278	14	-0.99
6229	0.527	-0.278	11	-1.54	
M62	6266	0.544	-0.264	62	-1.28
M9	6333	0.614	-0.212	7	-1.78
M92	6341	0.626	-0.203	9	-2.24
6362	0.535	-0.272	7	-1.08	
6402	0.564	-0.249	31	-1.39	
6426	0.665	-0.177	4	-2.20	
M28	6626	0.565	-0.248	6	-1.44
M22	6656	0.651	-0.186	8	-1.75
6712	0.557	-0.254	7	-1.01	
M54	6715	0.551	-0.259	31	-1.42
6723	0.540	-0.268	24	-1.09	
M55	6809	(0.620)	-0.208	2	-1.82
6934	0.545	-0.264	30	-1.54	
M72	6981	0.552	-0.258	26	-1.54
7006	0.567	-0.246	54	-1.59	
M15	7078	0.640	-0.194	27	-2.15
M2	7089	0.636	-0.197	13	-1.62
M30	7099	0.698	-0.156	3	-2.13

which is the mean¹ of the two least-squares solutions made by exchanging the dependent and the independent variables. The correlation coefficient is $r = 0.85$.

This correlation between period and metallicity is in the same sense as that found from the earlier star-by-star analysis of RR Lyrae stars in individual clusters (S82a). The smaller slope of 0.09 for this ensemble average, compared with 0.12 found from the star-by-star correlations, is expected because the distribution of individual variables along the HB in the Oosterhoff II clusters (M15-like, with long mean periods) is shifted more toward the blue (shorter periods within the strip) compared with type I clusters (M3-like, with short mean periods). This difference in the HB density distribution as a function of metallicity makes the ensemble average of the periods in a given Oosterhoff type II cluster smaller than the star-by-star average in the same cluster, which, of course, is independent of the weighting by the number density within the strip, whereas Figure 1 and equation (1) depend directly on it.

¹ One could argue about which, in fact, should be made the independent variable in this correlation. Because both ordinate and abscissa are subject to error ($[Fe/H]$ because of measuring errors; $\log \langle P_{ab} \rangle$ because of averaging over a finite sample), the average of the two least-squares solutions made by exchanging the variables is a reasonable estimate of the correlation (cf. footnote 2 of S90). In any case, the two solutions are nearly the same when the correlation coefficient, r , is high. They are identical when $r = 1$.

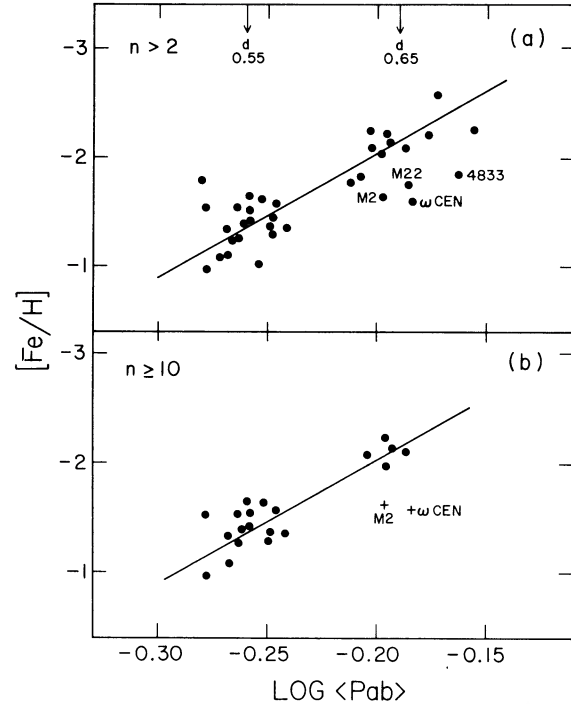


FIG. 1.—(a) Correlation of the mean period of RRab variables with metallicity for the clusters listed in Table 1 that have data for more than two variables. The four marked clusters which have the largest deviation to the right of the correlation line have extremely blue horizontal branches (resembling M13), suggesting appreciable post-ZAHB luminosity evolution that lengthens the periods of individual variables. (b) Same as (a), but for clusters with 10 or more RRab variables. The Oosterhoff period dichotomy is due to the absence of RR Lyrae stars in clusters of intermediate metallicity caused by the nonmonotonic tracking of the HB morphology with $[Fe/H]$ (Renzini 1983; Castellani 1983).

The reason for the gap in Figure 1 which causes the Oosterhoff dichotomy concerns why the horizontal branches which produce the required L/M ratios that go with these periods give no stars within the variable star strip when $[Fe/H]$ is in the narrow range between -1.6 and -2.0 . The clue must be connected with how $[Fe/H]$ and a second (unknown) parameter determine the morphology of the HB. Castellani, Giannone, and Renzini (1970, Fig. 12), Renzini (1983, Fig. 1) and Castellani (1983, Fig. 6) began the demonstration that has subsequently shown that as $[Fe/H]$ decreases through intermediate metallicities, with M13, NGC 2808, and NGC 6752 as examples, the distribution of stars along their horizontal branches shifts far to the blue and largely out of the variable star instability strip. But, as the metal abundance decreases still further, the HBs move back through the strip, again producing variable stars (cf. footnote 5 of S90). Because L and M , and therefore $L/M^{0.81}$, which controls the periods, are functions of $[Fe/H]$, no variable stars exist that have these particular $\langle L/M^{0.81} \rangle$ values, giving, thereby, the period gap in Figure 1.

We note again that $[Fe/H]$ is not the sole parameter that governs the HB morphology because (1) the morphology does not change monotonically with $[Fe/H]$ and (2) there are clusters on each side of the empty period range in Figure 1 that have the same value of $[Fe/H]$, yet have different mean RR Lyrae periods. Hence, some additional parameter(s) as well as $[Fe/H]$ must have an effect on the L/M ratio that controls the period at a given temperature. Despite the lack of a real under-

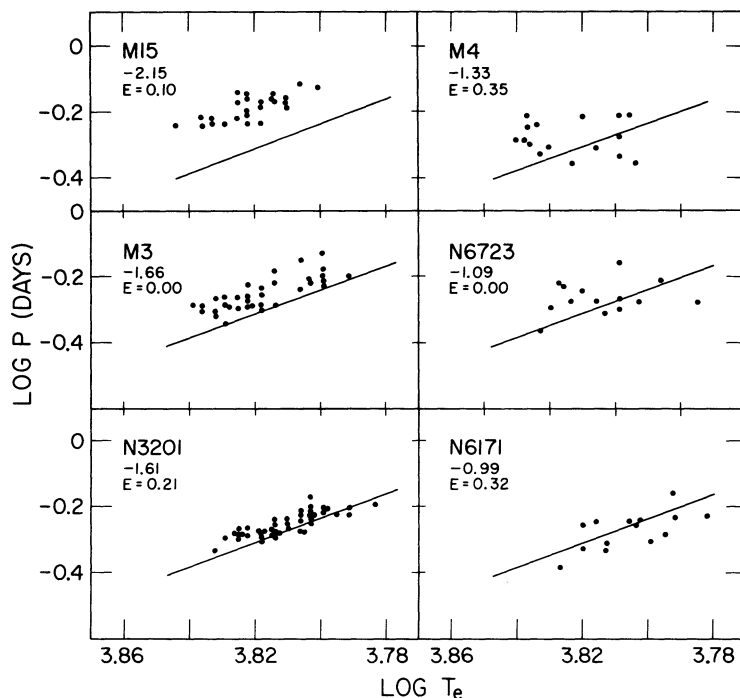


FIG. 2.—Period-temperature relations for program clusters studied earlier (Sandage 1990). The clusters are ordered by the metallicity shown in the code for each panel, which also shows the adopted reddening. The lower envelope line to the M3 data is repeated in each panel.

standing of why the HB morphology changes as it does, producing the multivalued variation of the red-to-blue ratio with $[\text{Fe}/\text{H}]$, this operational explanation of the period dichotomy by Renzini and by Castellani seems convincing. Their picture is, then, that the two Oosterhoff period groups are due to the nonmonotonic behavior of the HB morphology as $[\text{Fe}/\text{H}]$ and a second parameter are changed.

III. PERIOD SHIFTS AS A FUNCTION OF METALLICITY FOR GLOBULAR CLUSTER ZERO-AGE HORIZONTAL BRANCHES

We now come to the heart of the matter by showing the star-by-star nature of the period shifts. The period-temperature relations for six of the clusters studied in the preceding paper (S90) are shown in Figure 2 from data listed in the tables there. The fiducial line drawn in each panel is the lower envelope to the M3 distribution. Deviations in period from this line, read vertically at a given temperature, define the period shift $\Delta \log P(T_e)$ at constant temperature.

For the purposes of determining the period shifts star by star and cluster by cluster, the placement of this envelope line need not coincide with the zero-age horizontal-branch position for M3, but need only be parallel to it. This is because we can obtain the period-shift data for each star in a given cluster (relative to any adopted fiducial line) from which a mean period shift (i.e., the individual period shifts averaged over all variables in a given cluster) can be determined. It is the differences between these mean period shifts which are important. Clearly, such differences between clusters are independent of the placement of the fiducial period-temperature line.

To the extent that the mean of these period-shift differences is determined from fair samples in a given cluster (and neglecting the nearly inconsequential [for this purpose] change in evolutionary width of the HB with metallicity found in the preceding paper), the values will represent the period-shift dif-

ferences between the zero-age horizontal branches of one cluster relative to another. This assumption is expected to be an adequate first approximation concerning shifts of ZAHBs in lieu of precise data (because of small sample size) of the position of the true ZAHB in Figure 2. (The M3 envelope line as drawn, although close to the true ZAHB position, must be displaced from it by a small amount because of errors in T_e .)

But as a check on the above assumption that using mean period shifts adequately estimates the period-shift differences of the ZAHBs between clusters, we have approximated the problem in another (more direct) way of assuming that the three stars of shortest period at a given temperature in each of the 10 clusters discussed in the preceding paper themselves define the position of the ZAHB. Said differently, we are approximating the position of the ZAHB by the envelope line in the period-temperature diagram that passes near these stars in each cluster. Justification for this assumption (given the complication caused by varying sample size for the different clusters) is that the RR Lyrae luminosity function is peaked at the ZAHB (the stars spend most of their time there), making it more probable that the three faintest variables at a given T_e are near the ZAHB than would otherwise be the case (because of varying sample size) if the luminosity function were symmetrical.

There is general agreement, now to be set out, of the conclusions using both methods to approximate the position of the ZAHB from the limited RR Lyrae samples in each cluster. This agreement is the reason to believe that we are discussing adequate approximations to the correlations of the ZAHB itself, where, then, most of the effects of post-ZAHB evolution, discussed in the preceding paper, have been accounted for.

An elaborate statistical calculation for each cluster to locate the "true" ZAHB envelope lines in Figure 2 for each cluster could, of course, be made, as suggested by the referee. Here one

TABLE 2A
PERIOD SHIFTS AND MASS-TO-LIGHT RATIOS OF THE ZAHBs

Cluster (1)	[Fe/H] (2)	$E(B-V)$ (3)	$\log(L/M^{0.81})$ (4)	$\Delta \log P(T_e)$ (5)
M92	-2.25	0.02	1.871	+0.082
M15	-2.15	0.10	1.860	+0.076
M3	-1.66	0.00	1.772	0.000
NGC 3201	-1.61	0.21	1.752	-0.018
ω Cen	-1.59	0.11	1.811	+0.035
NGC 6981	-1.54	0.04	1.716	-0.051
M4	-1.33	0.35	1.693	-0.066
NGC 6723	-1.09	0.00	1.724	-0.042
NGC 6712	-1.01	0.42	1.680	-0.081
NGC 6171	-0.99	0.32	1.701	-0.063

TABLE 2B
MEAN MASS-TO-LIGHT RATIOS FOUND BY AVERAGING $\log(L/M^{0.81})$
VALUES FOR INDIVIDUAL VARIABLES IN THE PROGRAM CLUSTERS

Cluster (1)	[Fe/H] (2)	n (3)	$\langle \log(L/M^{0.81}) \rangle$ (4)	SD (5)
M92	-2.25	5	1.899	0.024
M15	-2.15	24	1.918	0.007
M3	-1.66	34	1.831	0.007
NGC 3201	-1.61	43	1.798	0.004
NGC 6981	-1.54	17	1.788	0.013
M4	-1.33	15	1.821	0.023
NGC 6723	-1.09	14	1.803	0.020
NGC 6712	-1.01	6	1.770	0.053
NGC 6171	-0.99	14	1.757	0.014

would use a statistical model involving sample sizes and the form of the HB luminosity function. However, such a formal analysis, given the uncertainties in the problem, would scarcely warrant a stronger confidence in the answer than our use of the two types of estimates here, one based on the three stars in each cluster of shortest period at a given temperature and the other using the *mean* period shifts, or the equivalent analysis using the *mean* values of the $L/M^{0.81}$ ratios, cluster to cluster.

Averaging the individual $\log(L/M^{0.81})$ as well as the period-shift values for the three stars closest to the ZAHB gives the data in columns (4) and (5) of Table 2A. The metallicities in column (2) are from Zinn and West (1984). The adopted reddenings in column (3) are those used in the preceding paper. The column (4) values are calculated from the pulsation equation

$$\log(L/M^{0.81}) = (\log P + 3.48 \log T_e - 11.497)/0.84 \quad (2)$$

of van Albada and Baker (1971), using the period and temperature data for each RR Lyrae variable in each cluster. Note from this equation that if we had adopted the slope of the period-temperature relation in Figure 2 to be -3.48 rather than -3.70 , then the $\Delta \log P(T_e)$ period deviations read in Figure 2 at constant temperature would be identical to $0.84 \Delta \log(L/M^{0.81})$. The values in columns (4) and (5) of Table 2A are, therefore, highly correlated. Clearly, the analysis via the period shifts at constant temperature is equivalent to that via the L/M ratio, because both are based on equation (2). This, of course, is why the conclusions of Caputo, Castellani, and di Gregorio (1983, Figs. 1, 2, and 3) using the L/M ratios are the same as those obtained from the somewhat less trans-

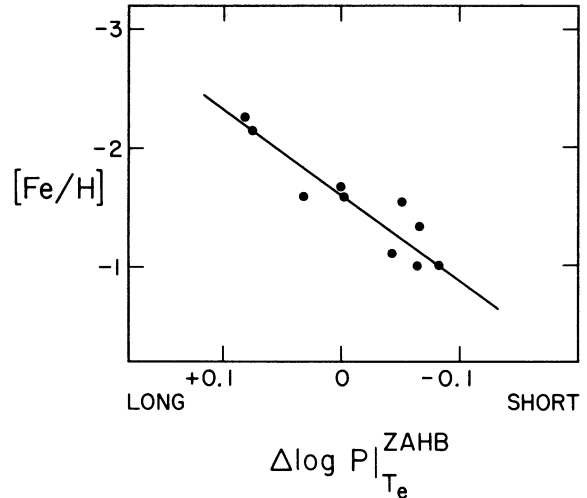


FIG. 3.—Correlation between metallicity and the RR Lyrae period shift at constant temperature for an approximation to the ZAHB of the 10 clusters listed in Table 2A.

parent method of the period shifts (SKS; S81, S82a) themselves.

The data in Table 2A are plotted in Figures 3 and 4. These diagrams illustrate what is seen directly in Figure 2, that the progressive period shift relative to the M3 envelope is a function of $[Fe/H]$. The least-squares solution for the correlation in Figure 3, taking $\Delta \log P(T_e)$ as the independent variable and using all 10 clusters in Table 2A, is

$$\Delta \log P(T_e) = -0.12[Fe/H] - 0.20, \quad (3)$$

with a high correlation coefficient of $r = 0.91$. It is to be noted that this solution has the same slope as was found in the first analysis of the problem (S81, S82a).

The least-squares regression for the data in Figure 4, taking $\log(L/M^{0.81})$ as the independent variable, is

$$\log(L/M^{0.81}) = -0.14[Fe/H] + 1.54, \quad (4)$$

with, of course, the same correlation coefficient of $r = 0.91$. As expected, the slopes in equations (3) and (4) are in the ratio of 0.84 as required by equation (2). This result shows straight-

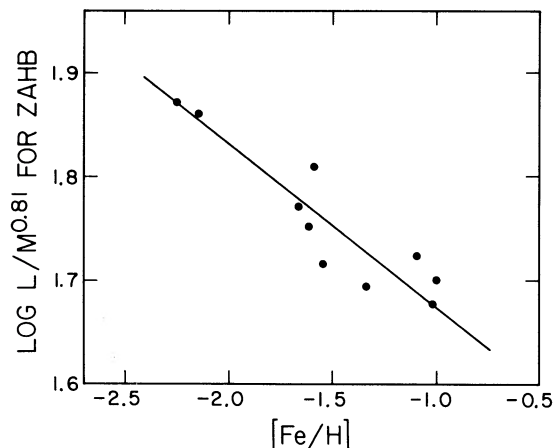


FIG. 4.—Correlation of the $L/M^{0.81}$ ratio with metallicity for an approximation to the ZAHB of the 10 clusters listed in Table 2A.

away that the two methods, one via period shifts and the other via equation (2) to calculate $\log(L/M^{0.81})$ by use of the temperatures directly, are equivalent.

To counter objections that use of the three stars of smallest period at a given temperature to define the ZAHB is sample-size-dependent, we have done the analysis with the mean values of $\log(L/M^{0.81})$ calculated using *all the variables* in each cluster, as discussed in the paragraphs above. The data are set out in Table 2B. The value of $\langle \log(L/M^{0.81}) \rangle$, averaging over all available RRab variables in each cluster, is given in column (4). The standard deviation of this mean is in column (5). The number of variables in each sample is in column (3).

The least-squares solution for the correlation of $\langle \log(L/M^{0.81}) \rangle$ with $[\text{Fe}/\text{H}]$, taking $\langle \log(L/M^{0.81}) \rangle$ as the independent variable, is

$$\langle \log(L/M^{0.81}) \rangle = -0.11[\text{Fe}/\text{H}] + 1.65, \quad (4a)$$

with a correlation coefficient of 0.90. This equation is similar to equation (4), although the slope is slightly smaller and the zero point is brighter because of post-ZAHB evolution. The difference in zero point between equations (4) and (4a), read at $[\text{Fe}/\text{H}] = -1.6$, is 0.16 mag, with equation (4a) being brighter. We consider equation (4a) to be better defined for the ZAHB than equation (4) owing to the use of more data, and we later adopt an equation very close to it (eq. [16]), except for a small downward change of zero point, due to post-ZAHB evolution, for the description of the ZAHB.

The reality of the correlations in Figures 3 and 4 and the data in Tables 2A and 2B depend on the correctness of the reddening corrections (Caputo 1988). To destroy the correlations requires systematic errors in temperature if one wishes to make each data set coincide with the M3 lower envelope in Figure 2 by horizontal shifts. For M15 this temperature error must be $\Delta \log T_e = 0.02$, requiring the true temperature to be cooler than we have adopted. Because the slope of the color-temperature calibration is $\Delta(B-V) = 3 \Delta \log T_e$, this requires an error in the reddening of $\Delta E(B-V) = 0.06$ mag. A reddening error of this size for M15 and for M92 is unlikely because of the high weight determination of $E(B-V)$ for each cluster from photoelectric photometry of the HB stars directly (Sandage 1969). In addition, a reddening error of 0.06 mag in the opposite direction would be required for the data in both NGC 6171 and M4 if we were to reduce their listed period shifts in column (5) to zero.

The adopted reddening for NGC 6171 of $E(B-V) = 0.32$ is based on photoelectric photometry with both the Mount Wilson 2.5 m reflector and the Palomar 5 m Hale telescope. The total photoelectric sample consists of 23 cluster stars and 19 field stars. Discussion of the data (Sandage and Roques 1984) accounted for a UV excess of the field stars and the expected gravity effect on the *UBV* colors for the NGC 6171 HB stars. A reddening as high as 0.38 mag was considered to be unlikely. The reddening adopted by Dickens (1970) of 0.28 mag is in the direction of *steepening* the slope in equations (3) and (4) rather than reducing them toward zero.

The mean reddening of M4, $\langle E(B-V) \rangle = 0.35$ mag, is adopted from Table 9 of the preceding paper (S90), based on the photoelectric data of Sturch (1977) and of Cacciari (1979) for the variables. There is some evidence for differential reddening over the field of a size of ~ 0.02 mag, as determined by Cacciari directly from the variables that are spread over the entire field of the cluster. The tightness of the vertical subgiant branch at $V = 13.5$ in the color-magnitude diagram by Lee

(1976, Figs. 4 and 5) and by Alcaino and Liller (1984, Fig. 6) precludes differential reddening much larger than this. The reddening of Zinn (1980) is $E(B-V) = 0.37$ mag, which again is not large enough to reduce the slopes of Figures 3 and 4 to zero. It seems unlikely, therefore, that 0.06 mag can be applied to M15 and M92 stars to make them redder, and 0.06 mag in the opposite direction to NGC 6171, NGC 6723, and M4 to make them bluer, so as to eliminate the correlation as required by Caputo (1988, Fig. 4b).

However, the slopes can be changed if the reddenings are changed systematically (within observational bounds) as a function of $[\text{Fe}/\text{H}]$. We now inquire what systematic error in $E(B-V)$ with metallicity is required to reduce the slope $d \log \Delta P(T_e)/d[\text{Fe}/\text{H}]$ to the value -0.049 predicted by Lee, Demarque, and Zinn (1988, 1990) in their evolutionary model for the period-shift correlation.

Suppose that the adopted reddening value for a particular cluster is changed by $\Delta E(B-V)$, thereby changing the $\log T_e$ values. The period-shift numbers will change by the following amount: The slope of the adopted (cf. Fig. 2 of S90) color-temperature relation is $d(B-V) = 2.9d \log T_e$ for the relevant temperature range and $[\text{Fe}/\text{H}]$ values of the RR Lyrae stars. This temperature error translates to an error in period of $d \log P = -3.7d \log T_e$, determined from the slope of the period-temperature relation. Hence, an error of $\Delta E(B-V)$ in reddening translates into an error in the period shift of $\Delta \log P(T_e) = 1.28\Delta E(B-V)$.

Evidently, then, based on equation (3), the slope in Figure 3 can be reduced to -0.049 predicted by LDZ by introducing the progressive error of $\Delta E(B-V) = 0.055\Delta[\text{Fe}/\text{H}]$ in the reddenings of the 10 program clusters. The extent to which this progressive error is reasonable can be judged by adopting an independent set of $E(B-V)$ values for the Table 2A clusters and testing therefrom the effect on the Figure 3 correlation. To this end we use the reddenings determined by Zinn (1980).

Zinn's reddening values, in the order set out in Table 2A, are 0.03, 0.08, 0.02, 0.27 [value for ω Cen omitted], 0.07, 0.37, 0.05, 0.39, and 0.38 mag, compared with our adopted values of 0.02, 0.10, 0.00, 0.21, 0.11, 0.04, 0.35, 0.00, 0.42, and 0.32 mag for M92, M15, M3, NGC 3201, ω Cen, NGC 6981, M4, NGC 6723, NGC 6712, and NGC 6171, respectively. For each cluster the difference in reddening, $\Delta E(B-V)$, between Zinn's values and those we have adopted has been computed, from which the corrections of $1.28\Delta E(B-V)$ to the $\log T_e$ values were made to the period-shift values. In a similar way, corrections to $\log(L/M^{0.81})$ were made from equation (2) directly.

Using these independent reddenings by Zinn gives a revised correlation for Figure 3 of $\Delta \log P(T_e) = -0.095[\text{Fe}/\text{H}] - 0.131$, with a reduced correlation coefficient of $r = 0.70$, using all 10 clusters. (A slope of -0.061 is obtained by excluding NGC 6712.) The corresponding slope for the luminosity-to-mass ratio in Figure 4 is $d \log(L/M^{0.81})/d[\text{Fe}/\text{H}] = -0.117$, again using all the data, or -0.086 excluding NGC 6712.

Therefore, it seems unlikely that reasonable changes in the reddening can reduce the slopes of Figures 3 and 4 to zero, and somewhat improbable that such changes can be made to give the LDZ slope for Figure 3 of -0.049 and -0.058 for Figure 4. However, because of the many attractive features of the model by Lee, Demarque, and Zinn, we inquire further into the value of the period-shift-metallicity slope by using Lub's data on field RR Lyrae stars of different metallicity to see whether we can obtain the smaller LDZ slope.

IV. L/M RATIOS AND PERIOD SHIFTS FOR RR LYRAE FIELD STARS

The variation of the Oosterhoff mean period with metallicity, discovered by Arp (1955), is seen in RR Lyrae field star data as well as in the clusters, both in the L/M ratio (Lub 1977, 1987) and in the period shifts at constant amplitude (Preston 1959, Fig. 5; S82*b*, Fig. 1). In this section we discuss the field star correlations in more detail than was possible before Lub's data were available.

In a preliminary analysis of his data, Lub (1987, Fig. 5) used the temperature scale based on his calibration of the Walraven photometry together with his photometric measurement of $[\text{Fe}/\text{H}]$, obtaining the tight correlation of the luminosity-to-mass ratio and metallicity of

$$\log(L/M^{0.81}) = -0.10[\text{Fe}/\text{H}] + 1.74. \quad (5)$$

He further showed that this correlation for the field stars was followed by the globular clusters M15, ω Cen, and M4 as well, using the photoelectric data of de Bruyn and Lub (1986) and of Bingham *et al.* (1984).

Equation (5) should be compared with equations (4) and (4a) of § III, which are based on our *cluster* sample from Tables 2A and 2B but where the temperature scale was determined from $(B-V)_{\text{mag}}$ colors rather than directly using the more precise Walraven photometry obtained by Lub. But to make the field variables and the cluster data (Figs. 3 and 4) compatible for comparison, we have repeated the analysis of Lub's field star data by treating the temperatures (and therefore the period shifts at constant T_e) and the $\log(L/M^{0.81})$ ratio with the methods used in the last section. To this end, we list in Table 3 the relevant parameters for the field stars, based on Lub's (1977) extensive photometry and data tables.

The metallicities set out in column (3) are calculated from Lub's photometric blanketing index $\Delta[B-L]$ (in units of \log_{10} of intensity ratio) using his calibration of

$$[\text{Fe}/\text{H}] = -2.15 + 21\Delta[B-L], \quad (6)$$

given as equation (14) of his thesis (Lub 1977, p. 111). The $\Delta[B-L]$ blanketing index values (Lub 1979) which we used are listed in Table 2A of Lub (1977, p. 104). Column (4) gives the blue amplitude (in magnitudes) obtained from Lub's (1977, Table 1) values of A_V (in log intensity units), to which is added $A_B - A_V$ (in log intensity units read from the $V-B$ color curves of Lub 1977, pp. 21–55, also in log intensity units). The result is then multiplied by 2.5. Column (5) lists the average color $\langle B-V \rangle_{\text{mag}}$ (the angular brackets being Lub's notation for an average taken over the color curve kept in log intensity units), calculated by multiplying the values of $\langle V-B \rangle$ from column (13) of Lub's Table 1 by 2.5. This type of color average taken over the log of the intensity ratios was shown by Preston (1961), and in § IV of the preceding paper, to be the appropriate color to use to obtain the temperature of the equivalent static star. [The $B-V$ color system of the Walraven photometry as measured by Lub is very close to the Johnson $B-V$ system, seen by comparing the $2.5(V-B)$ values at minimum light that are tabulated by Lub 1977 in his Table 3 with the measurements of the minimum light colors by Sturch 1966, Table 4, for stars in common.]

The reddenings in column (6) of Table 3 are on the Johnson $B-V$ photometric system obtained from

$$E(B-V)_j = 2.1E(V-B)_w, \quad (7)$$

where $E(V-B)_w$ is the reddening (in log intensity units) measured on the Walraven system (Lub 1977, Table 2A). The factor 2.1 is read from Lub and Pel's (1977, Fig. 7) diagram that compares the two reddening systems.

Subtracting column (6) from column (5) (with the result not shown) and using the color-temperature calibration in § III of S90 gives the temperatures listed in column (7). Columns (8), (9), and (10) show the $L/M^{0.81}$ ratios and the period shifts at constant temperature and at constant amplitude relative to the M3 fiducial period-temperature and period-amplitude lower envelope lines, obtained in the manner described in previous sections.

The period-temperature relation from columns (2) and (7) is shown in Figure 5*b*. Temperatures determined directly by Lub (1977, Table 3A, pp. 149–150) from his calibration of the Walraven photometry are shown in Figure 5*a*, transformed from his θ_e values by $T_e = 5040/\theta_e$. To be consistent with the analysis of the period shifts given in S90 and in sections of the present paper, we use the temperature scale in column (7) that is based on the $(B-V)_{\text{mag}}$ colors.

Consider first the $\log(L/M^{0.81})$ values in column (8) obtained from the column (7) temperature scale of Table 3. The correlation between columns (3) and (8) is shown in Figure 6, similar to Figure 5 of Lub (1987) but now on the same temperature scheme as Figures 3 and 4 above. The least-squares correlation, omitting the deviant stars HH Pup, XX Vir, AN Ser, AT Ser, and DX Del, is

$$\log(L/M^{0.81}) = -0.10[\text{Fe}/\text{H}] + 1.704, \quad (8)$$

which is virtually identical with equation (5) despite our different ways of treating the temperatures.

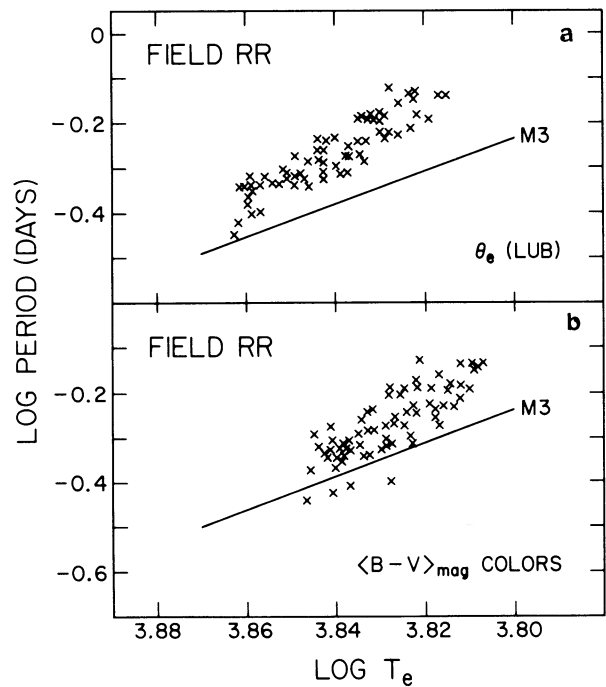


FIG. 5.—Period-temperature relation for the field RR Lyrae stars studied by Lub (1977). (a) Lub's temperatures determined from his calibration of the Walraven photometry. (b) Temperatures determined from Lub's $\langle B-V \rangle_{\text{mag}}$ colors (averaged over magnitudes, not intensities) read from the color-temperature relation used elsewhere (Sandage 1990). The M3 lower envelope is repeated in each panel.

TABLE 3
LUB'S DATA FOR FIELD RRab LYRAE STARS

Name (1)	log P (2)	[Fe/H] (3)	A_B (4)	$\langle B-V \rangle$ mag (5)	$E(B-V)$ (6)	log T_c (7)	log $L/M^{0.81}$ (8)	$\Delta \log P(T)$ (9)	$\Delta \log P(A)$ (10)
RY Psc	-0.276	-1.33	1.13	0.343	0.017	3.829	1.848	+0.068	+0.005
W Tuc	-0.192	-1.62	1.46	0.325	0.006	3.828	1.943	+0.149	+0.131
RR Cet	-0.257	-1.44	1.24	0.353	0.025	3.827	1.862	+0.080	+0.038
SS For	-0.305	-1.50	1.74	0.295	0.011	3.841	1.863	+0.084	+0.054
RZ Cet	-0.292	-1.42	1.29	0.328	0.021	3.835	1.853	+0.075	+0.009
X Ari	-0.186	-2.15	1.33	0.483	0.141	3.812	1.884	+0.095	+0.121
SV Eri	-0.146	-1.79	0.90	0.395	0.032	3.808	1.915	+0.121	+0.105
U Pic	-0.356	-0.85	1.66	0.348	0.036	3.839	1.794	+0.025	-0.007
U Lep	-0.236	-1.75	1.41	0.333	0.029	3.832	1.908	+0.119	+0.081
RY Col	-0.320	-0.91	1.01	0.363	0.025	3.829	1.795	+0.024	-0.055
IU Car	-0.132	-1.86	1.26	0.450	0.086	3.807	1.928	+0.131	+0.166
HH Pup	-0.408	-1.08	1.82	0.435	0.126	3.837	1.724	-0.034	-0.038
BB Pup	-0.318	-0.79	1.36	0.438	0.092	3.828	1.793	+0.023	-0.008
WY Ant	-0.241	-1.54	1.23	0.363	0.029	3.824	1.868	+0.085	+0.053
AF Vel	-0.278	-1.67	1.30	0.438	0.113	3.825	1.829	+0.052	+0.025
TV Leo	-0.172	-1.86	1.62	0.345	0.019	3.822	1.942	+0.146	+0.172
W Crt	-0.385	-0.70	1.75	0.353	0.055	3.846	1.788	+0.022	-0.024
SS Leo	-0.203	-1.67	1.47	0.333	0.017	3.828	1.930	+0.138	+0.122
ST Leo	-0.321	-1.27	1.75	0.330	0.040	3.841	1.844	+0.068	+0.040
X Crt	-0.135	-1.73	0.86	0.373	0.017	3.812	1.945	+0.146	+0.111
UU Vir	-0.323	-1.10	1.50	0.330	0.027	3.838	1.829	+0.055	+0.005
SV Hya	-0.320	-1.52	1.66	0.335	0.059	3.844	1.857	+0.080	+0.029
AV Vir	-0.182	-1.33	1.03	0.388	0.019	3.814	1.897	+0.107	+0.086
RV Oct	-0.243	-1.88	1.49	0.463	0.139	3.822	1.858	+0.075	+0.084
FY Hya	-0.196	-2.15	1.50	0.345	0.036	3.825	1.926	+0.134	+0.133
V 499 Cen	-0.283	-1.67	1.61	0.368	0.063	3.832	1.852	+0.072	+0.060
UY Boo	-0.187	-1.98	1.54	0.338	0.015	3.821	1.920	+0.128	+0.147
XX Vir	+0.130	-1.84	1.60	0.368	0.038	3.820	2.294	+0.441	--
TY Aps	-0.300	-1.65	1.36	0.465	0.137	3.823	1.794	+0.022	+0.010
TV Lib	-0.569	-0.53	1.71	0.350	0.061	3.852	1.749	-0.010	-0.083
FW Lup	-0.315	-0.49	0.58	0.480	0.099	3.823	1.776	+0.007	-0.105
VY Ser	-0.146	-1.79	0.98	0.400	0.032	3.809	1.919	+0.124	+0.115
AR Ser	-0.240	-1.65	1.20	0.373	0.029	3.818	1.845	+0.064	+0.050
VY Lib	-0.273	-1.37	1.46	0.510	0.149	3.817	1.801	+0.027	+0.050
AN Ser	-0.282	0.12	1.47	0.415	0.042	3.832	1.853	+0.073	+0.043
AT Ser	-0.127	-1.79	1.24	0.338	0.006	3.821	1.992	+0.188	+0.168
AV Ser	-0.312	-1.69	1.50	0.485	0.172	3.828	1.801	+0.029	+0.016
UV Oct	-0.266	-1.71	1.64	0.410	0.092	3.827	1.851	+0.071	+0.081
V4450ph	-0.401	-0.22	1.27	0.628	0.242	3.828	1.695	-0.060	-0.102
VX Her	-0.342	-1.58	1.72	0.355	0.074	3.841	1.819	+0.047	+0.015
RW Tra	-0.427	-0.18	1.13	0.488	0.145	3.341	1.717	-0.038	-0.146
V4520ph	-0.254	-1.75	1.31	0.525	0.183	3.817	1.824	+0.046	+0.050
ST Oph	-0.340	-1.50	1.79	0.525	0.221	3.834	1.785	+0.017	+0.026
V494 Sco	-0.369	-1.06	1.35	0.448	0.151	3.840	1.782	+0.016	-0.060
TY Pav	-0.148	-2.13	1.18	0.440	0.086	3.808	1.913	+0.119	+0.139
V690 Sco	-0.308	-0.93	1.52	0.448	0.118	3.837	1.843	+0.066	+0.023
S Ara	-0.345	-1.54	1.74	0.395	0.107	3.839	1.807	+0.036	+0.014
V 675 Sgr	-0.192	-1.98	1.28	0.405	0.074	3.818	1.902	+0.112	+0.108
V 455 Oph	-0.343	-1.44	1.19	0.425	0.113	3.833	1.784	+0.016	-0.054
V 413 Cra	-0.230	-1.63	0.96	0.445	0.095	3.816	1.848	+0.066	+0.029
V 440 Sgr	-0.321	-1.48	1.64	0.403	0.103	3.837	1.827	+0.053	+0.026
DN Pav	-0.329	-1.58	1.70	0.343	0.050	3.837	1.818	+0.045	+0.025
V 341 Aql	-0.238	-1.31	1.64	0.355	0.038	3.832	1.905	+0.117	+0.109
AA Aql	-0.442	-0.83	1.78	0.358	0.065	3.846	1.720	-0.035	-0.077
DX Del	-0.326	-0.09	1.05	0.440	0.057	3.830	1.792	+0.022	-0.056
RV Cap	-0.349	-1.39	1.23	0.320	0.046	3.847	1.835	+0.062	-0.055
V Ind	-0.319	-1.52	1.74	0.338	0.042	3.837	1.829	+0.055	+0.040
CP Aqr	-0.334	-0.85	1.70	0.358	0.046	3.841	1.828	+0.055	+0.020
SW Aqr	-0.338	-1.48	1.74	0.343	0.046	3.837	1.807	+0.036	+0.021
Z Mic	-0.231	-1.48	0.90	0.485	0.118	3.813	1.835	+0.054	+0.020
SX Aqr	-0.271	-1.84	1.50	0.320	0.044	3.841	1.903	+0.118	+0.058
RT Gru	-0.291	-1.56	1.51	0.323	0.050	3.844	1.892	+0.109	+0.039
TZ Aqr	-0.243	-1.42	1.12	0.400	0.053	3.822	1.858	+0.075	+0.036
RW Cru	-0.259	-1.67	1.51	0.300	0.002	3.834	1.888	+0.104	+0.168
BH Peg	-0.193	-1.65	0.92	0.458	0.107	3.815	1.888	+0.100	+0.061
BO Aqr	-0.159	-1.79	1.51	0.370	0.029	3.817	1.937	+0.141	+0.171
YY Tuc	-0.197	-1.84	1.55	0.323	0.004	3.825	1.925	+0.133	+0.138
DN Aqr	-0.198	-1.65	1.04	0.368	0.006	3.810	1.862	+0.076	+0.071
RV Phe	-0.224	-1.58	0.98	0.368	0.023	3.819	1.868	+0.083	+0.037
BR Aqr	-0.317	-0.81	1.52	0.348	0.023	3.835	1.824	+0.050	+0.014
UU Cet	-0.217	-1.58	0.95	0.398	0.038	3.812	1.847	+0.064	+0.041

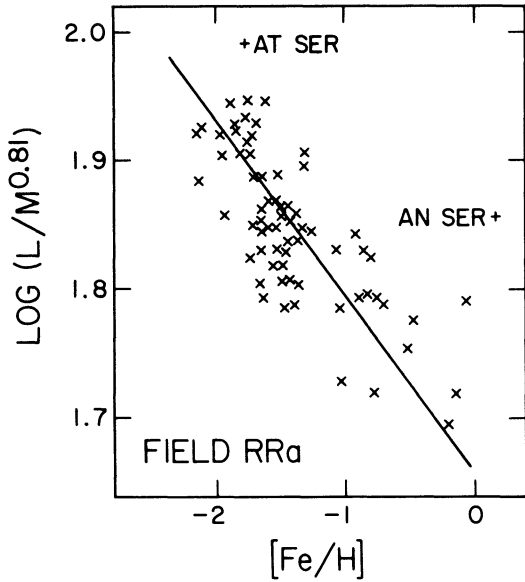


FIG. 6.—Correlation of the metallicity and $L/M^{0.81}$ for the field RR Lyrae stars listed in Table 3.

Although Figure 6 shows that the correlation is definite, the fine structure in the diagram (the clump near $[\text{Fe}/\text{H}] \sim -1.6$) suggests potential problems. Lub mentions a problem with the $\log g$ determinations which, in turn, may affect our adopted color-temperature relation (Y.-W. Lee 1989, private communication). For this reason, we inquire next into the period shifts at constant amplitude which are independent of temperature and therefore of $\log g$; this, of course, then opens

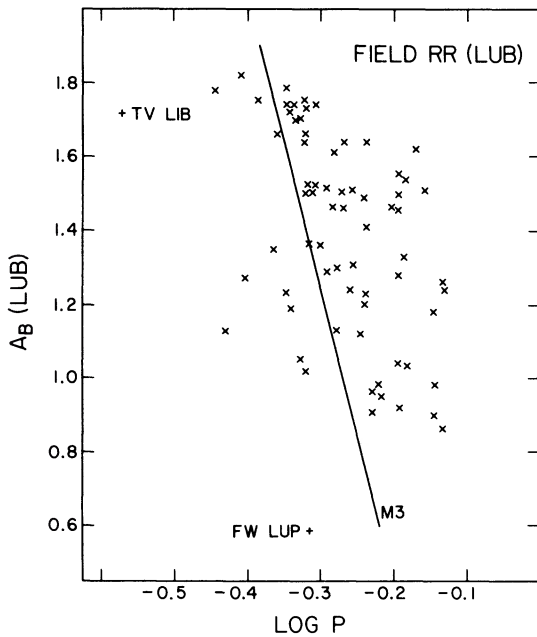


FIG. 7.—Period-amplitude data for the field RR Lyrae stars studied by Lub, as listed in Table 3. The line is the envelope of shortest period at a given amplitude for variables in M3. This line, whose equation is $\log P = -0.129A_B - 0.135$, is the fiducial from which we have measured period shifts at constant amplitude. For the purposes of the argument, it need not be the line of the ZAHB in its zero point.

the discussion to the Caputo (1988) effect, i.e., that the amplitude may vary with $[\text{Fe}/\text{H}]$, for which we shall later correct.

Figure 7 shows the period-amplitude relation plotted from the data in columns (2) and (4) of Table 3. The M3 fiducial envelope line is shown, whose equation (S90, Appendix A) is

$$\log P = -0.129A_B = -0.135. \quad (9)$$

The period shifts at constant amplitude, listed in column (10) of Table 3, are determined from the horizontal displacements from this line.

The data from columns (3) and (10) of Table 3 are plotted in Figure 8b. These are compared in Figure 8a with the period shifts at constant temperature that are taken from column (9) of Table 3. As discussed earlier, Figure 8a is equivalent to the correlation of $0.84 \log(L/M^{0.81})$ with $[\text{Fe}/\text{H}]$ in Figure 6 (note the reversal between abscissa and ordinate between these two diagrams). The slope of the correlation in Figure 8a is

$$d \Delta \log P(T_e) / d[\text{Fe}/\text{H}] = -0.08, \quad (10)$$

which is, then, equivalent to $d \log(L/M^{0.81}) / d[\text{Fe}/\text{H}] = -0.10$. The least-squares regression in Figure 8b between the period shift at constant amplitude and $[\text{Fe}/\text{H}]$ is

$$\Delta \log P(A_B) = -0.13[\text{Fe}/\text{H}] - 0.15, \quad (11)$$

with a correlation of $r = 0.81$.

Suppose, now, that the correlation found by Caputo for the ω Cen variables between amplitude and $[\text{Fe}/\text{H}]$ (at a given period) of

$$\Delta(A_B) = 0.34[\text{Fe}/\text{H}] + 0.67 \quad (12)$$

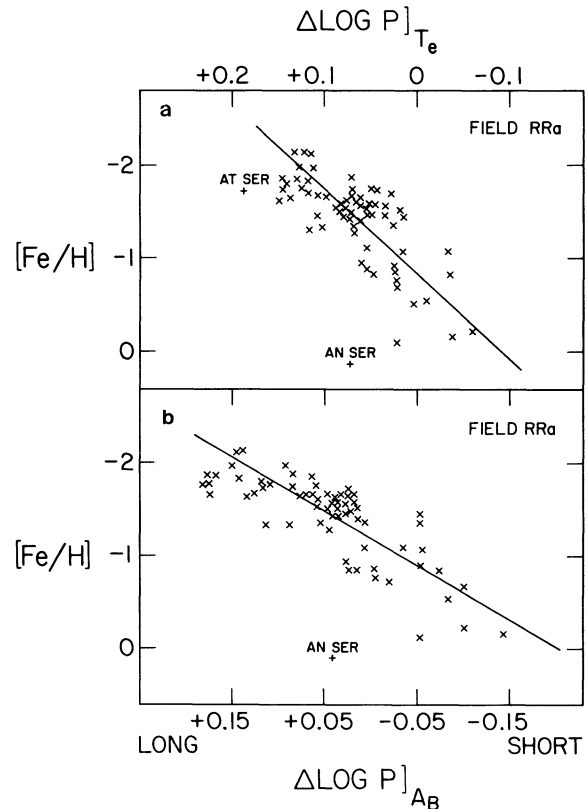


FIG. 8.—Correlation of metallicity with the period shifts (a) at constant temperature and (b) at constant amplitude, from the data for the field variables listed in Table 3.

applies to all variables. The effect is to reduce the slope in equation (11) in the following way. The period-amplitude fiducial line for M3 from equation (9) shows that reducing the amplitude (at a given period) using the recipe of equation (12) will reduce the period shift at constant amplitude by $(0.129)(0.34) = 0.044$ in $\Delta \log P(A_B)$. Hence, the slope in equation (11), corrected for the Caputo (1988) effect, will be

$$d \Delta \log P(A_B(\text{corr}))/d[\text{Fe}/\text{H}] = -0.09. \quad (13)$$

It is, then, fair to summarize the field star data as follows. The correlations of the luminosity-to-mass ratio with metallicity for both the *cluster* (Fig. 4 and eqs. [4] and [4a]) and the *field star* (Fig. 6 and eq. [5]) data have similar slopes. The corresponding slopes of the equivalent $\Delta \log P(T_e)$, $[\text{Fe}/\text{H}]$ correlations (Figs. 3 and 8a, representing eqs. [3] and [11]) average $\Delta \log P(T_e)/d[\text{Fe}/\text{H}] = -0.10$. This value is twice as large as the predicted slope of -0.05 of the LDZ evolutionary model. Confirmation that the larger slope is correct is available from equation (13), where the slope of -0.09 is corrected for the Caputo effect, and where the determination is independent of questions of uncertainties in the reddening and temperature values.

We finally note that the period shifts for the *field variables* are due to the combination of (1) the effect of evolution away from the ZAHB and (2) the variation with metallicity of the luminosity-to-mass ratio of the ZAHB itself. The period shifts due to post-ZAHB luminosity evolution cause horizontal scatter (at a given metallicity) in Figures 8a and 8b and vertical scatter in Figure 6. The size of the scatter should equal the range of period shifts seen in the individual clusters studied previously (S90). The ranges found there depend on $[\text{Fe}/\text{H}]$, but they average about $\langle \Delta \log P \rangle = 0.15$. This is close to the observed range in $\Delta \log P(T_e)$ at a given metallicity in Figure 8, and its equivalent in Figure 6, caused by the range in the RR Lyrae luminosity of ~ 0.4 mag at constant $[\text{Fe}/\text{H}]$. On the other hand, the *systematic* variation with metallicity of the *ridgeline* period shifts in Figures 3 and 8 and the luminosity-to-mass ratio in Figures 4 and 6 is caused by the variation of the luminosity of the ZAHB itself with $[\text{Fe}/\text{H}]$, as we show in the next section.²

V. LUMINOSITY OF THE ZAHB AS A FUNCTION OF $[\text{Fe}/\text{H}]$

Using any of the versions of equations (4), (4a), (5), and (8) for $\log(L/M^{0.81}) = f([\text{Fe}/\text{H}])$, or their equivalent form of $1.19 \Delta \log P(T_e) = f([\text{Fe}/\text{H}])$ from equations (3), (10), and (13), we can set out the resulting predictions of how $M_{\text{bol}}(\text{RR})$ changes with $[\text{Fe}/\text{H}]$ once assumptions are made about RR Lyrae star masses. The various solutions obtained in the last section,

² As an aside we note, with the referee, that if the field halo variables are physically similar to those in globular clusters, then the dispersion in the period-temperature relation in Fig. 5b should be the same as that in the data set that is the sum of all the cluster data, of which the six panels in Fig. 2 are a subset. This would be strictly true if the mix of $[\text{Fe}/\text{H}]$ values was the same for the cluster sample and the field sample. We have tested for the similarity of the dispersions in our samples by comparing the standard deviations (SDs) of the totality of the $\Delta \log P(T_e)$ period shifts at constant temperature listed in col. (9) of Table 3 for the field stars with the SD of the sum of the same quantity for the six clusters in Fig. 2, using the data in the relevant columns in Tables 4, 5, 6, 8, 9, and 10 of S90 for the cluster variables. The SD of the field star data, i.e., the measure of the spread from the M3 envelope line in Fig. 5b, is $\text{SD}[\Delta \log P(T_e)] = 0.050$. The summed cluster data for the six clusters in Fig. 2 gives $\text{SD}[\Delta \log P(T_e)] = 0.057$. The two values are clearly the same to within the uncertainty introduced by the nonidentical distributions of $[\text{Fe}/\text{H}]$ of the two samples.

together with two independent solutions by Cacciari *et al.* (1985; see eq. [15] below) and Cacciari (private communication; see eq. [16] below), are

$$\log(L/M^{0.81}) = -0.10[\text{Fe}/\text{H}] + 1.74 \quad (\text{eq. [5]}),$$

which is Lub's ridgeline for field stars;

$$\log(L/M^{0.81}) = -0.10[\text{Fe}/\text{H}] + 1.70 \quad (\text{eq. [8]}),$$

which is the ridgeline from our analysis of Lub's field star data;

$$\log(L/M^{0.81}) = -0.14[\text{Fe}/\text{H}] + 1.54 \quad (\text{eq. [4]}),$$

which was assumed to apply to the ZAHB of globular clusters (Table 2A, Fig. 4, or a similar correlation from the data in Table 2B and eq. [4a]);

$$\log(L/M^{0.81}) = -0.14[\text{Fe}/\text{H}] + 1.58, \quad (14)$$

which is the lower envelope to the field star data in Figure 6;

$$\log(L/M^{0.81}) = -0.08[\text{Fe}/\text{H}] + 1.72, \quad (15)$$

which is the ridgeline from Cacciari *et al.*'s (1985) analysis of nine globular clusters; and

$$\log(L/M^{0.81}) = -0.09[\text{Fe}/\text{H}] + 1.68, \quad (16)$$

which is the ridgeline determined by Cacciari from 23 field RR Lyraes which have excellent temperatures determined from $V-K$ colors. Equation (16) is expected to be the most accurate of the above solutions.

The difference in zero point between the two groups of these solutions (i.e., ridgeline versus lower envelopes) exists, obviously, because ridgelines refer to the mean RR Lyrae luminosity, made brighter by evolution away from the zero-age horizontal branch, whereas lower envelopes refer to the ZAHB level itself. The zero-point difference between equations (4a) and (8) at $[\text{Fe}/\text{H}] = -1.6$ is 0.10 mag, which is close to the value expected from the standard deviation of the width of the observed HBs in clusters studied in the preceding paper (S90, Table 13). The difference in slope between the two groups (-0.14 for the ZAHB and -0.08 to -0.10 for the ridgelines), if significant, suggests that the off-ZAHB evolution tends to lower the L/M dependence on metallicity. (I am indebted to C. Cacciari for suggesting the summary and the remarks in the previous two paragraphs.)

To obtain luminosities from the above equations, we now must discuss the RR Lyrae masses as a function of $[\text{Fe}/\text{H}]$. If all variables have the same mass, the bolometric magnitudes based on equations (4), (5), (8), (14), (15), and (16) would vary with $[\text{Fe}/\text{H}]$ with slope coefficients of $dM_{\text{bol}}/d[\text{Fe}/\text{H}]$ of 0.25, 0.25, 0.35, 0.35, 0.20, and 0.22, respectively. We show (Sandage and Cacciari 1990) in the following paper that the bolometric correction is

$$\text{BC} = 0.06[\text{Fe}/\text{H}] + 0.06, \quad (17)$$

which reduces the dependence of $M_V(\text{RR})$ on $[\text{Fe}/\text{H}]$ in these same equations to 0.19, 0.19, 0.29, 0.29, 0.14, and 0.16, respectively, in the *constant-mass* case.

The assumption that the mass is independent of $[\text{Fe}/\text{H}]$, however, is probably incorrect. Three investigations suggest that RR Lyrae star masses become larger as the stars become more metal-poor.

1. Consider first the theory of the zero-age horizontal branch. The expectation from the canonical models of Rood (1970), and of Sweigart and Gross (1976), confirmed by the

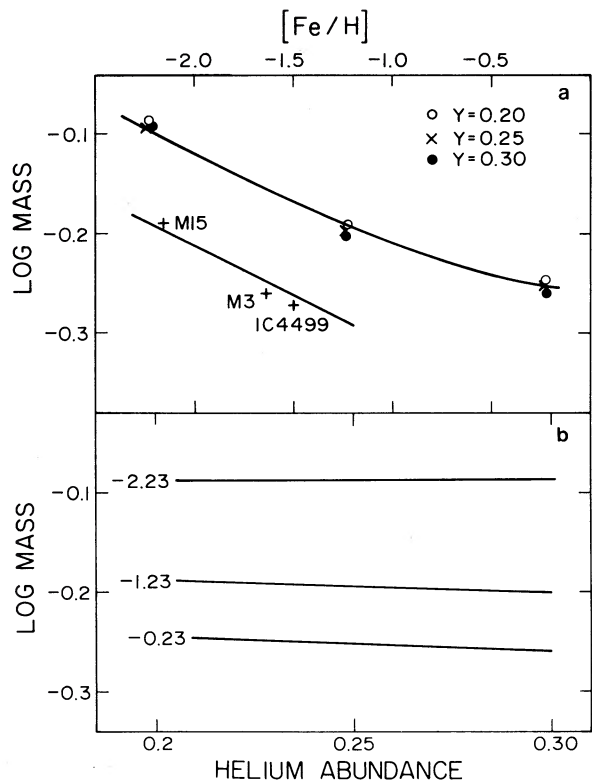


FIG. 9.—Variation of the RR Lyrae mass with chemical composition. (a) Predicted sensitivity of the mass (at $\log T_e = 3.85$) to $[\text{Fe}/\text{H}]$ and Y from the ZAHB models of Sweigart, Renzini, and Tornambè (1987, Table 1) shown as open circles, filled circles, and plus signs, compared with the observed mass as a function of metallicity from the double-mode variables in three clusters. (b) The same theoretical predictions from the SRT models as in (a), but displayed as a function of Y for different $[\text{Fe}/\text{H}]$ values.

extensive new models of SRT, is that mass varies with metallicity according to

$$\log M = -0.10[\text{Fe}/\text{H}] - 0.318 \quad (18)$$

over the range of $[\text{Fe}/\text{H}] < -1.0$, nearly independent of the helium abundance. The predictions from these models, taken from the tables of SRT, are shown in Figure 9a as open and closed circles and crosses for $\log T_e = 3.85$. Figure 9b shows the independence of the mass with variations of Y , but again illustrating the strong variation of the ZAHB mass with $[\text{Fe}/\text{H}]$.

2. Also shown in Figure 9a are the calculations of mass from the double-mode RR Lyrae stars in M15 (SKS), in IC 4499 (Clement *et al.* 1986), and in M3 (see Cox 1987 for a review). The calculation of the double-mode masses by Cox, Hodson, and Clancy (1983) follows the development of the double-mode theory by Stellingwerf (1975b), Petersen (1978, 1979), and Cox, King, and Hodson (1980). The result, fitted through the three cluster points in Figure 9a, is

$$\log M = -0.10[\text{Fe}/\text{H}] - 0.41, \quad (19)$$

which has the same slope as the SRT models but is displaced from them by $\Delta \log M = 0.092$ toward smaller masses. However, some caution must be expressed concerning these masses from the double-mode calculations. Both Cacciari (1989, private communication) and Lee, Demarque, and Zinn (1990) point out that not enough is yet known about the sensitivity of the double-mode mass values that are derived from the

Petersen diagram to changes in the adopted opacities and to changes in $[\text{Fe}/\text{H}]$. Some of the problems are set out by Cox (1987), where he shows, among other things, that the calculations by Kovács (1985) give a different zero point than is shown in Figure 9a for the cluster data calculated by Cox, Hodson, and Clancy (1983), simply by using a different pulsation code and opacity values for a given $[\text{Fe}/\text{H}]$. Furthermore, if the mass calculation is sensitive to changes in $[\text{Fe}/\text{H}]$, the mass difference between M15 and the two more metal-rich clusters in Figure 9a (M3 and IC 4499) might decrease (the Petersen diagram for the double-mode results has been calculated only for one chemical composition) as it has for the classical Cepheids. Because equation (19) is a keystone upon which conclusions concerning $M_V(\text{RR}) = f([\text{Fe}/\text{H}])$ can be made to depend, which in turn affect the age of the globular cluster system (Sandage and Cacciari 1990), it is important that these theoretical uncertainties eventually be removed by more detailed calculations of the Petersen diagram.

3. The evolutionary model of LDZ predicts a mass variation that is intermediate between equation (19) and the case of no dependence on metallicity, giving

$$\log \langle M \rangle = -0.053[\text{Fe}/\text{H}] - 0.235, \quad (20)$$

based on ZAHB starting masses that are similar to those of SRT from equation (18). The smaller slope in equation (20) than in equation (18) expresses the fact that the LDZ assumed evolution takes stars redward from their starting positions on the ZAHB. Stars at such blueward starting positions have smaller masses than those at more redward positions on the ZAHB.

Equations (5), (8), and (16) appear to be the most reliable representations of the observations. With the various mass possibilities discussed above, equation (5), which we adopt, can be transformed as follows.

Consider first the case of constant mass. Using the results from the Baade-Wesselink calibration of absolute magnitude for 22 field stars, together with equation (5), used now in reverse to determine M , gives $\langle M \rangle = 0.555 M_\odot$, independent of $[\text{Fe}/\text{H}]$ (C. Cacciari 1989, private communication). Using this mass (as a given), put back into equation (5) to obtain M_{bol} , and using the bolometric magnitude of the Sun to be +4.75 together with the bolometric correction of equation (17), gives

$$M_V(\text{RR}) = 0.86 + 0.19[\text{Fe}/\text{H}]. \quad (21)$$

To be sure, this simply recovers input values of $M_V(\text{RR})$ obtained directly from the Baade-Wesselink determinations of the 22 program stars summarized by Cacciari, but the absolute magnitude in equation (21) would be independent of this circular argument if we could use any other method (such as averaging the observations in Fig. 9a, lower curve) that would give a constant $\langle M \rangle = 0.55 M_\odot$ for the mass.

Consider next the mass in equation (19) from the double-mode calculations. This, combined with equations (5) and (17), gives

$$M_V(\text{RR}) = 1.17 + 0.39[\text{Fe}/\text{H}]. \quad (22)$$

Consider, finally, the mass from equation (20) given by LDZ from their evolutionary model. Although this model seems to be inconsistent with the observed slope of the period-shift- $[\text{Fe}/\text{H}]$ correlation and therefore may not apply, this intermediate-mass case will nevertheless illustrate what the double-mode

mass method might eventually give when the calculations are made more complete, based on the concerns of Cox and of Kovács quoted earlier, centered on the effect of varying the metal abundance. Combining equations (5), (17), and (20) gives

$$M_V(\text{RR}) = 0.82 + 0.30[\text{Fe}/\text{H}] . \quad (23)$$

The zero points in equations (21), (22), and (23) depend on (1) the value of the adopted constant in equation (2) (given there as 11.497 from van Albada and Baker 1971), (2) the zero point of the adopted color-temperature calibration (S90), and (3) the zero points of the mass relations in equations (18), (19), and (20). These three types of zero points are uncertain enough (e.g., see Cox 1987, Table I, for the uncertainty in the pulsation constant) to make the zero point of equations (21), (22), and (23) uncertain by about 0.2 mag. It needs to be pointed out further that these equations refer to the *ridgeline* of the distributions. The values for the ZAHB (i.e., corrected for evolution) are ~ 0.1 mag fainter.

VI. THE THEORETICAL ZAHB MODELS REQUIRE Y AND $[\text{Fe}/\text{H}]$ TO BE ANTICORRELATED TO EXPLAIN THE PERIOD-SHIFT-METALLICITY AND THE L/M -METALLICITY RELATIONS IF THE OBSERVATIONS APPLY TO THE ZAHB

We now inquire how the observed metallicity dependence of the period shifts in equations (1), (3), (10), (11), and (13), or their $\log(L/M^{0.81})$ equivalents in equations (4), (4a), (5), (8), and (14)–(16), can be reconciled with the canonical ZAHB models. In an exhaustive discussion, SRT show how the theoretical period shifts depend on the masses, luminosities, and metallicities of model ZAHB stars. As mentioned earlier, both their results and those found earlier by others in the references quoted in § I show that the canonical ZAHB models require Y and Z to be anticorrelated. The purpose of the present section is to demonstrate this fact again by using diagrams that compare the model predictions with the observations in a different way.

Figure 1 of SRT shows the luminosity levels of ZAHBs for different Y and Z chemical abundances. The crucial parameter for the period-shift prediction is the mass of the model stars marked on each sequence. The period of an RR Lyrae pulsator on the ZAHB is calculated from equation (2) using the model values of L and M at, say, the fixed temperature of $\log T_e = 3.85$.

SRT show (their Fig. 4) that the predicted periods have virtually no dependence on Z but a very strong dependence on Y . Hence, because of the strong dependence of L and M on Z but the independence of M on Y (Fig. 9b), it is required that a change in Z be accompanied by an opposite change in Y to produce the observed period-shift-metallicity correlation.

The periods calculated by SRT from their model ZAHBs are too long by a factor of about 1.2 compared with real RR Lyrae stars, and their calculated $L/M^{0.81}$ values are too small by about the same factor (cf. Table 2A here, compared with Table 1 of SRT). These theoretical values of P and $L/M^{0.81}$ can be made to agree with the observations if the masses shown in Figure 3 of SRT are changed to agree with equation (19) in § V by just the shift between the two lines in Figure 9a.

By modifying the SRT mass- $[\text{Fe}/\text{H}]$ relation by this zero-point shift, we can calculate the predicted $L/M^{0.81}$ ratios from equation (2) using the model values of L and M (modified) listed by SRT at $\log T_e = 3.85$ (their Table 1). The results are set out in Table 4. Figure 10 shows these model predictions for

TABLE 4
ZAHB PARAMETERS FROM THE SRT MODELS^a

Z (1)	$[\text{Fe}/\text{H}]$ (2)	$\log L_{3.85}$ (3)	$M'_{3.85}$ (4)	$\log P_{3.85}$ (5)	$\log(L/M^{0.81})$ (6)
$Y_{\text{ms}} = 0.20$					
-2.23.....	0.0001	1.670	0.659	-0.374	1.818
-1.23.....	0.001	1.596	0.527	-0.371	1.821
-0.23.....	0.01	1.519	0.460	-0.395	1.793
$Y_{\text{ms}} = 0.25$					
-2.23.....	0.0001	1.735	0.664	-0.322	1.880
-1.23.....	0.001	1.658	0.520	-0.315	1.888
-0.23.....	0.01	1.594	0.454	-0.328	1.873
$Y_{\text{ms}} = 0.30$					
-2.23.....	0.0001	1.800	0.661	-0.266	1.946
-1.23.....	0.001	1.724	0.512	-0.255	1.960
-0.23.....	0.01	1.673	0.446	-0.257	1.957

^a Using masses based on double-mode observations.

$L_{3.85}$ for various Z (Fig. 10a) and Y (Fig. 10b) abundances. The interpolation equation for the $L(Y, Z)$ dependence shown in this diagram is

$$\log L_{3.85} = 1.3Y - 0.070[\text{Fe}/\text{H}] + 1.252 , \quad (24)$$

which is a satisfactory fit to within ~ 0.03 mag over the relevant range of Y and $[\text{Fe}/\text{H}]$.

It is now easy to show that the *predicted* period shift from the models is virtually zero as $[\text{Fe}/\text{H}]$ is varied (cf. also SRT, Fig. 4). Although at fixed Y the luminosity increases with

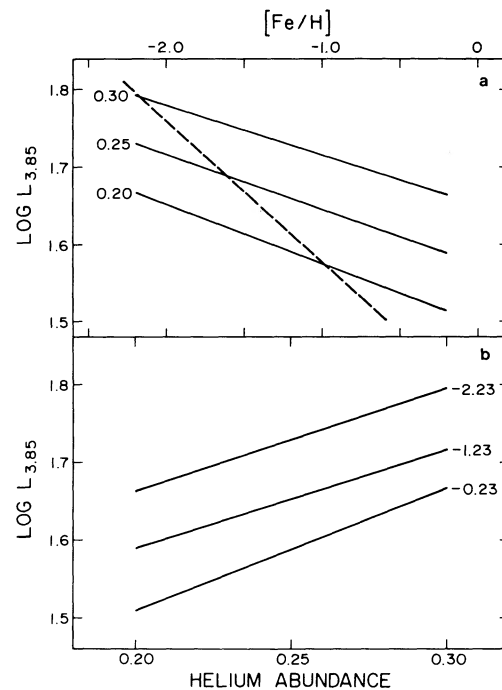


FIG. 10.—Predictions of RR Lyrae luminosity (at $\log T_e = 3.85$) from the SRT ZAHB models as functions of (a) $[\text{Fe}/\text{H}]$ and (b) Y , as listed in Table 4. The twofold dependence is described by eq. (24) of the text. The L - $[\text{Fe}/\text{H}]$ dependence required by the observations via the pulsation equations (found by combining eqs. [5] and [19]) is shown as a dashed line in (a).

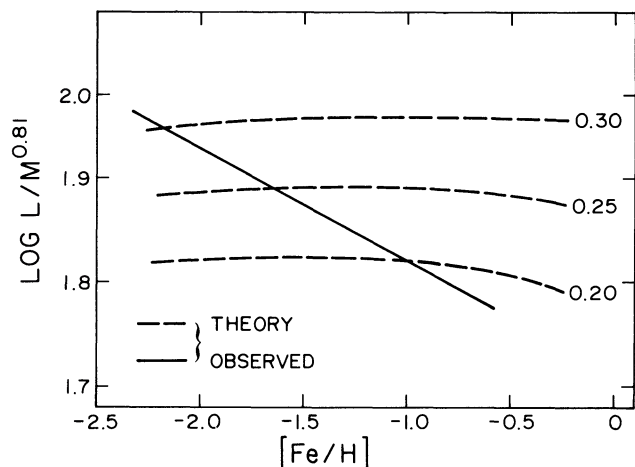


FIG. 11.—Predicted variation of $L/M^{0.81}$ with $[\text{Fe}/\text{H}]$ and Y from the ZAHB models of SRT from the data in Table 4. The observed variation is the solid line from eq. (5). The requirement for the anticorrelation of $[\text{Fe}/\text{H}]$ and Y is evident if ZAHB models apply.

decreasing metallicity (eq. [23] and Fig. 10), the mass also increases with decreasing metallicity (Fig. 9a). The two effects nearly cancel one another in the $L/M^{0.81}$ ratio, giving *no period shift* with $[\text{Fe}/\text{H}]$ for fixed Y . This is seen by merging equations (19) and (24) to give

$$\log(L/M^{0.81}) = 1.3Y + 0.011[\text{Fe}/\text{H}] + 1.584 \quad (25)$$

as the prediction from the model, showing that L/M is nearly independent of $[\text{Fe}/\text{H}]$ if Y is fixed.

The values of $L/M^{0.81}$ in Table 4 are plotted in Figure 11 as dashed lines at constant Y , with, again, equation (25) fitting the predicted values to better than ~ 0.03 mag over the relevant parameter range. The adopted variation of $L/M^{0.81}$ with $[\text{Fe}/\text{H}]$ from equation (5) is shown as a solid line in Figure 11. The needed anticorrelation of Y and Z to explain the observations using ZAHB models is evident. Its strength is obtained by combining equations (5) and (25) to give

$$\Delta Y = -0.09\Delta[\text{Fe}/\text{H}], \quad (26)$$

as the requirement, identical with the above-mentioned conclusion of SRT and Caputo, Castellani, and di Gregorio (1983), who studied the observations independently and by a different path through the equations. A theoretical model of the efficiency of deep mixing (VandenBerg and Smith 1988) as a function of metallicity suggests the possibility that about half the necessary correlation in equation (26) might actually occur.

The attractive feature of the evolutionary model of LDZ is the *elimination of the equation (26) requirement* for an anticorrelation. They suggest that the metal-poor RR Lyrae stars are *not* on the ZAHB, and therefore that such models do not apply to them. However, as emphasized earlier, their predicted period shifts and predicted masses are both smaller by a factor of 2 than the observations, continuing, therefore to block a satisfactory solution to this period-shift problem.

Despite the lack of a complete theoretical understanding via ZAHB models, the nevertheless definite conclusion from the present analysis is that the Oosterhoff-Arp correlation of mean period with metallicity for cluster variables (and the parallel correlation for the field variables) requires that the M_V values for the RR Lyrae stars depend on $[\text{Fe}/\text{H}]$ —a central fact which we use in the paper that follows.

I am indebted to Carl Cacciari for so carefully reading an early draft of this paper and for making important suggestions concerning the uncertainties, now outlined in § V, in the mass estimates for the variables and the effect of these uncertainties on the central issue of the slope of the $M_V(\text{RR})/[\text{Fe}/\text{H}]$ relation. I am also grateful to A. Sweigart, D. VandenBerg, and an unknown referee for comments that have resulted in a reshaping of some of the arguments. I am particularly indebted to Y.-W. Lee, P. Demarque, and R. Zinn for keeping me informed during the past several years of their calculations from their evolutionary model. Discussions between us of an early draft of this paper clarified a number of points concerning their objections to the present analysis, and my perceptions of their model. Although we still have not reached a common ground, the points at issue are now more clearly identified because of their comments during an important discussion between us that occurred in Boston in 1989 January.

REFERENCES

- Alcaino, G., and Liller, W. 1984, *Ap. J. Suppl.*, **56**, 19.
 Arp, H. C. 1955, *A.J.*, **60**, 317.
 Bingham, E. A., Cacciari, C., Dickens, R. J., and Fusi Pecci, F. 1984, *M.N.R.A.S.*, **209**, 765.
 Buonanno, R., Corsi, C. E., and Fusi Pecci, F. 1988, *Astr. Ap.*, **216**, 80.
 Cacciari, C. 1979, *A.J.*, **84**, 1542.
 Cacciari, C., Clementini, G., Fusi Pecci, F., and Lolli, M. 1985, *Mem. Soc. Astr. Italiana*, **56**, 97.
 Caloi, V., Castellani, V., and Tornambè, A. 1978, *Astr. Ap. Suppl.*, **33**, 169.
 Caputo, F. 1988, *Astr. Ap.*, **189**, 70.
 Caputo, F., Castellani, V., and di Gregorio, R. 1983, *Astr. Ap.*, **123**, 141.
 Caputo, F., Castellani, V., and Tornambè, A. 1978, *Astr. Ap.*, **67**, 107.
 Caputo, F., Cayrel, R., and Cayrel de Strobel, G. 1983, *Astr. Ap.*, **123**, 135.
 Caputo, F., DeStefanis, P., Paez, E., and Quarta, M. L. 1987, *Astr. Ap. Suppl.*, **68**, 119.
 Castellani, V. 1983, *Mem. Soc. Astr. Italiana*, **54**, 141.
 Castellani, V., Giannone, P., and Renzini, A. 1970, *Ap. Space Sci.*, **9**, 418.
 Clement, C. C., Dickens, R. J., and Bingham, E. E. 1979, *A.J.*, **84**, 217.
 Clement, C. M., Nemeč, J. M., Wells, N. R., Wells, T., Dickens, R. J., and Bingham, E. A. 1986, *A.J.*, **92**, 825.
 Cox, A. N. 1987, in *IAU Colloquium 95, Second Conference on Faint Blue Stars*, ed. A. G. D. Philip, D. S. Hayes, and J. W. Liebert (Schenectady: Davis), p. 161.
 Cox, A. N., Hodson, S. W., and Clancy, S. P. 1983, *Ap. J.*, **266**, 94.
 Cox, A. N., King, D. S., and Hodson, S. W. 1980, *Ap. J.*, **236**, 219.
 de Bruyn, J., and Lub, J. 1987, in *Stellar Pulsation*, ed. A. N. Cox, W. M. Sparks, and S. G. Starrfield (Lecture Notes in Physics, No. 274; Berlin: Springer-Verlag), p. 233.
 Dickens, R. J. 1970, *Ap. J. Suppl.*, **22**, 249.
 Gratton, R. G., Tornambè, A., and Ortolani, S. 1986, *Astr. Ap.*, **169**, 111 (GTO).
 Iben, I. 1971, *Pub. A.S.P.*, **83**, 697.
 Kinman, T. D. 1959, *M.N.R.A.S.*, **119**, 538.
 Kovács, G. 1985, *Acta Astr.*, **35**, 37.
 Lee, S.-W. 1976, *Astr. Ap. Suppl.*, **27**, 367.
 Lee, Y.-W., Demarque, P., and Zinn, R. 1988, in *Calibrating Stellar Ages*, ed. A. G. D. Philip (*Van Vleck Obs. Contr.*, No. 7; Schenectady: Davis), p. 149.
 ———. 1990, *Ap. J.*, **350**, 155.
 Lub, J. 1977, Ph.D. thesis, University of Leiden.
 ———. 1979, *A.J.*, **84**, 383.
 ———. 1987, in *Stellar Pulsation*, ed. A. N. Cox, W. M. Sparks, and S. G. Starrfield (Lecture Notes in Physics, No. 274; Berlin: Springer-Verlag), p. 218.
 Lub, J., and Pel, J. W. 1977, *Astr. Ap.*, **54**, 137.
 Oosterhoff, P. 1939, *Observatory*, **62**, 104.
 ———. 1944, *Bull. Astr. Inst. Netherlands*, **10**, 55.
 Petersen, J. O. 1978, *Astr. Ap.*, **62**, 205.
 ———. 1979, *Astr. Ap.*, **80**, 53.
 Preston, G. W. 1959, *Ap. J.*, **130**, 507.
 ———. 1961, *Ap. J.*, **133**, 29.
 Renzini, A. 1983, *Mem. Soc. Astr. Italiana*, **54**, 335.
 Renzini, A., and Fusi Pecci, F. 1988, *Ann. Rev. Astr. Ap.*, **26**, 199.
 Rood, R. T. 1970, *Ap. J.*, **161**, 145.
 Sandage, A. 1969, *Ap. J.*, **157**, 515.
 ———. 1981, *Ap. J.*, **248**, 161 (S81).
 ———. 1982a, *Ap. J.*, **252**, 553 (S82a).
 ———. 1982b, *Ap. J.*, **252**, 574 (S82b).

- Sandage, A. 1990, *Ap. J.*, **350**, 603 (S90).
Sandage, A., and Cacciari, C. 1990, *Ap. J.*, **350**, 645.
Sandage, A., Katem, B., and Sandage, M. 1981, *Ap. J. Suppl.*, **46**, 41 (SKS).
Sandage, A., and Roques, P. 1984, *Ap. J.*, **89**, 1166.
Sawyer Hogg, H. 1973, *Pub. David Dunlap Obs.*, Vol. 3, No. 6.
Stellingwerf, R. F. 1975a, *Ap. J.*, **195**, 441.
———. 1975b, *Ap. J.*, **199**, 705.
Sturch, C. 1966, *Ap. J.*, **143**, 774.
———. 1977, *Pub. A.S.P.*, **89**, 349.
- Sweigart, A. V., and Gross, P. G. 1976, *Ap. J. Suppl.*, **32**, 367.
Sweigart, A. V., Renzini, A., and Tornambè, A. 1987, *Ap. J.*, **312**, 762 (SRT).
Tornambè, A. 1985, *Mem. Soc. Astr. Italiana*, **56**, 85.
van Albada, T. S., and Baker, N. 1971, *Ap. J.*, **169**, 311.
———. 1973, *Ap. J.*, **185**, 477.
VandenBerg, D. A., and Smith, G. H. 1988, *Pub. A.S.P.*, **100**, 314.
Zinn, R. 1980, *Ap. J. Suppl.*, **42**, 19.
Zinn, R., and West, M. J. 1984, *Ap. J. Suppl.*, **55**, 45.

ALLAN SANDAGE: The Observatories of the Carnegie Institution of Washington, 813 Santa Barbara Street, Pasadena, CA 91101